Solitons in spiral polymeric macromolecules

A. V. Savin
State Institute of Physico-Technical Problems, ulica Prechistenka 13/7, 119034 Moscow, Russia

L. I. Manevitch
N. N. Semenov Institute of Chemical Physics, Russian Academy of Sciences, ulica Kosygina 4, 117977 Moscow, Russia
(Received 6 May 1999)

The problem of the existence and stability of dynamical soliton regimes in a helix polymer is solved numerically. For the polytetrafluoroethylene macromolecule, within a model in which deformations of the valence and torsion angles and the valence bonds are taken into account, two types of soliton solutions are found. The first type describes the propagation of a solitary wave of torsional displacements of a helix chain. The twisting of the chain is a result of the compression of dihedral (torsion) angles. The second type describes the propagation of a solitary wave of longitudinal displacements of a helix chain. The longitudinal compression of the chain is a result of the compression of the valence angles and bonds. The solitons have a finite narrow spectrum of supersonic velocities: the soliton of torsion has a spectrum above the velocity of long-wavelength phonons of torsion while the spectrum of the solitons of compression lies above the velocity of long-wavelength phonons of longitudinal displacement. Numerical simulations of the soliton dynamics show their stability in the intervals of admissible velocities. The elasticity of soliton interactions under their collisions is demonstrated. The formation of solitons induced by deformation of end bonds of the helix chain has been modeled. It is shown that helicity of the macromolecule is the necessary condition for existence of torsional solitons.

PACS number(s): 42.65.Tg, 63.20.Ry, 63.20.Pw

I. INTRODUCTION

The development of modern nonlinear physics has led to discovery of solitonic mechanisms determining at a molecular level the elementary events of many physical processes in crystals and other ordered molecular systems. Today, the role of supersonic solitons, ensuring the most efficient mechanism of energy transport in molecular systems with quasi-one-dimensional structure, is quite clear [1–4]. A supersonic soliton (nonlinear solitary wave) in such systems usually presents a moving molecular local field of longitudinal deformation (for instance, an α-helix molecule of a protein [5–7]).

From the very beginning [8–11] until now the basic model for studying nonlinear dynamics is an anharmonic one-dimensional lattice. However, real molecular chains are three dimensional and it is necessary to take account of not only longitudinal but also transverse displacements of the chain. Numerical modeling of the soliton dynamics in nonlinear networks has shown a high sensitivity of the excitations to the transverse perturbations [12,13].

The ground state of a molecular chain in space is the three-dimensional helix. A model of the helix chain as a natural generalization of the one-dimensional Fermi-Pasta-Ulam model was studied in Ref. [7]. The authors supposed that the structure of the helix was stabilized by the pair interactions of three nearest-neighbor molecules of the chain. The modeling of the nonlinear dynamics of concrete molecular chains requires using more realistic potentials taking into account the strain of valence bonds and the changes of valence and conformational angles.

To the present time the macromolecule polyethylene (PE) $(CH_2—)_x$ has been the most investigated in the class of polymeric macromolecules [14–19], each segment of which consists of one carbon atom. The ground state of this molecule is the plane zigzag conformation corresponding to the 1*2/1 spiral. The regularity of the zigzag chain leads to essential peculiarities of its dynamics, but for the majority of macromolecules of the class considered the ground state is not a plane zigzag, but a three-dimensional helix. Therefore it is also interesting to consider the nonlinear dynamics of a macromolecule having in the ground state the shape of a three-dimensional spiral.

The macromolecule polytetrafluoethylene (PTFE) $(CF_2—)_x$ in the ground state has the shape of a three-dimensional 1*13/6 spiral. The objective of the present work is to study the solitary waves dynamics in an isolated spiral macromolecule. It will be shown that the helicity of the chain leads to the existence of a specific type of localized excitations—supersonic solitons, (solitary waves) of torsion. Thus, in a spiral macromolecule there can be two different types of supersonic solitons providing the propagation of localized longitudinal and torsion strains of a spiral (in contrast to a plane zigzag, where only supersonic solitons of the first type can exist). For the molecule PTFE the spectrum of velocities of supersonic solitons is found and their dynamic properties are investigated.

The importance of the study of the nonlinear dynamics of helix chains is connected also with the appearance of experimental work in this field [20]. It is clear now that experimental data related to the behavior of crystalline PTFE at high temperatures can be explained by the formation of localized solitonlike torsional excitations. So the significant question arises as to whether localized torsional excitations stipulated by intramolecular interactions can exist in an isolated helix chain. An alternative possibility is the dominating role of

intermolecular interactions in this connection (similarly to the case of crystalline PE).

II. THE MODEL

The molecule PTFE in the crystalline state has a spiral conformation 1*13/6 with lattice periods $a=b=0.559$ nm, $c=1.688$ nm [21]. We accept further the approach of ''united atoms'' (i.e., we consider the CF_2 group as a single particle with mass $M=50m_p$, where m_p is the mass of a proton).

Let us consider a chain of PTFE. Then in the equilibrium state the nth site of the chain will be described by a position vector

$$\mathbf{R}=(R_0\cos(n\Delta\phi),R_0\sin(n\Delta\phi),n\Delta\phi), \tag{1}$$

where R_0 is the radius, $\Delta\phi=12\pi/13=166.15°$ the angular step, and $\Delta z=c/13=0.1298$ nm the longitudinal step of the spiral.

The length of the valence bond C—C $\rho_0=0.1533$ nm. It follows from the formula (1) that the squared length of the valence bond is

$$\rho_0^2=|\mathbf{R}_{n+1}-\mathbf{R}_n|=2R_0^2[1-\cos(\Delta\phi)]+\Delta z^2,$$

so that the spiral radius

$$R_0=\sqrt{(\rho_0^2-\Delta z^2)/2[1-\cos(\Delta\phi)]}=0.410\ \text{Å}.$$

In the equilibrium state the valence angle $\angle$CCC has the value

$$\theta_0=\arccos[-(\mathbf{e}_{n-1},\mathbf{e}_n)/\rho_o^2],$$

where the vector $\mathbf{e}_n=\mathbf{R}_{n+1}-\mathbf{R}_n$ has the direction of the nth valence bond. After transformations we obtain

$$\theta_0=\pi-\arccos\{[4R_0^2\sin^2(\Delta\phi/2)\cos\Delta\phi+\Delta z^2]/\rho_0^2\}$$
$$=116.30°.$$

The equilibrium value of the dihedral (torsional) angle is

$$\eta_n=\arccos[(\mathbf{v}_{n-1},\mathbf{v}_n)/|\mathbf{v}_{n-1}||\mathbf{v}_n|]$$
$$=\arccos\left(\frac{h^2\cos\Delta\phi+\sin^2\Delta\phi}{h^2+\sin^2\Delta\phi}\right),$$

where $\mathbf{v}_n=[\mathbf{e}_n,\mathbf{e}_{n+1}]$ is the cross product of vectors $\mathbf{e}_n,\mathbf{e}_{n+1}$ and $h=\Delta z/R_0$ is the dimensionless longitudinal step of the spiral. Further, we use the angle of rotation around the nth valence bond $\delta_n=\pi-\eta_n$ where η_n is the nth dihedral angle. In the equilibrium state the angle of rotation is

$$\delta_0=\pi-\eta_0=16.32°.$$

Let x_n, y_n, and z_n be the coordinates of the nth united atom of the helix backbone. After transformation from the Cartesian frame to the cylindrical one,

$$x_n=(R_0+r_n)\cos(n\Delta\phi+\varphi_n),$$

$$y_n=(R_0+r_n)\sin(n\Delta\phi+\varphi_n),$$

$$z_n=n\Delta z+h_n$$

(r_n is the transverse, φ_n the angular, and h_n the longitudinal displacement of the nth site of the chain from the equilibrium state), the Hamiltonian of the chain looks like

$$H=\sum_n\{\tfrac{1}{2}M[\dot r_n^2+\dot\varphi_n^2(R_0+r_n)^2+\dot h_n^2]$$
$$+V(\rho_n)+U(\theta_n)+W(\delta_n)\}, \tag{2}$$

where the overdot denotes the derivative with respect to time t, ρ_n is the length of the nth valence bond, and θ_n and δ_n are the nth valence and rotational angles, respectively.

The potential of a valence bond is given by

$$V(\rho_n)=D_0\{1-\exp[-\alpha(\rho_n-\rho_0)]\}^2,$$

where the length of the nth bond is

$$\rho_n=[a_{n,1}+b_n^2]^{1/2}.$$

Here,

$$a_{n,1}=d_n^2+d_{n+1}^2-2d_nd_{n+1}c_{n,1},$$

$$b_n=\Delta z+h_{n+1}-h_n,$$

$$d_n=R_0+r_n,$$

$$c_{n,1}=\cos(\Delta\phi+\varphi_{n+1}-\varphi_n).$$

The energy of a valence bond is $D_0=334.72$ kJ/mol and the parameter $\alpha=19.1\ \text{nm}^{-1}$ [22].

The energy of a valence angle is

$$U(\theta_n)=\tfrac{1}{2}K_\theta[\cos(\theta_n)-\cos(\theta_0)]^2,$$

where the value of the nth valence angle

$$\theta_n=\arccos[-(a_{n,2}+b_{n-1}b_n)/\rho_{n-1}\rho_n].$$

Here,

$$a_{n,2}=d_{n-1}d_nc_{n-1,1}+d_nd_{n+1}c_{n,1}-d_n^2-d_{n-1}d_{n+1}c_{n,2},$$

$$c_{n,2}=\cos(2\Delta\phi+\varphi_{n+1}-\varphi_{n-1}).$$

According to [18], the energy $K_\theta=529$ kJ/mol.

The potential of an internal rotation $W(\delta_n)$ characterizes the deformation caused by the rotation around the nth valence bond. The value of the nth rotational angle is

$$\delta_n=\arccos[-(b_nb_{n+1}a_{n,2}+b_{n-1}b_na_{n+1,2}-b_n^2a_{n,4}$$
$$-b_{n-1}b_{n+1}a_{n,1}+a_{n,3}a_{n+1,3})/\sqrt{\beta_n\beta_{n+1}}],$$

where

$$a_{n,3}=d_{n-1}d_ns_{n-1,1}+d_nd_{n+1}s_{n,1}-d_{n-1}d_{n+1}s_{n,2},$$

$$a_{n,4}=d_nd_{n+2}c_{n+1,2}-d_nd_{n+1}c_{n,1}-d_{n-1}d_{n+2}c_{n,3}$$
$$+d_{n-1}d_{n+1}c_{n,2},$$

$$s_{n,1}=\sin(\Delta\phi+\varphi_{n+1}-\varphi_n),$$

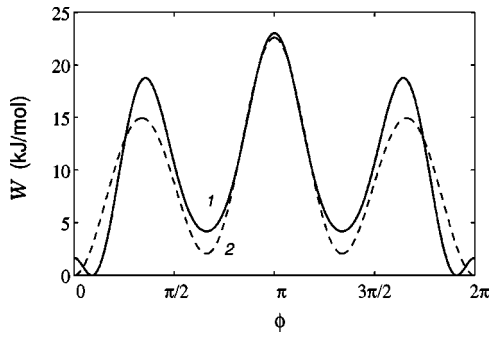

FIG. 1. Potential of rotation around the valence bond C—C $W(\delta)$ for macromolecules PTFE (curve 1) and PE (curve 2).

$$s_{n,2}=\sin(2\Delta\phi+\varphi_{n+1}-\varphi_{n-1}),$$

$$c_{n,3}=\cos(3\Delta\phi+\varphi_{n+2}-\varphi_{n-1}),$$

$$\beta_n=a_{n-1,1}b_n^2+a_{n,1}b_{n-1}^2-2a_{n,2}b_{n-1}b_n+a_{n,3}^2.$$

The expression (2) is also the Hamiltonian for a zigzag PE chain. It is possible to take the mass $M=14m_p$, the valence angle $\theta_0=113°$, and the rotational (conformational) angle $\delta_0=0$ [the spiral has radius $R_0=\rho_0\cos(\theta_0/2)/2=42.3$ pm, longitudinal step $\Delta z=\rho_0\sin(\theta_0/2)=0.1278$ nm, and angular step $\Delta\phi=\pi$].

III. POTENTIAL OF INTERNAL ROTATION

The potential of the internal rotation for the macromolecule PE is shown in Fig. 1. An absolute minimum of the potential $\delta_0=0$ corresponds to the *trans* conformation, and the other two minima to *gauche* conformations. The potential is characterized by three characteristics: the height of the potential barrier between *trans* and *gauche* conformations, the second minimum of the potential $\epsilon_2=U(2\pi/3)$ corresponding to the energy of a *gauche* conformation, and the maximal value $\epsilon_3=U(\pi)$ related to the energy level of the shadowed conformation. In accordance with [21] $\epsilon_1=14.94$ kJ/mol, $\epsilon_2=2.0768$ kJ/mol, and $\epsilon_3=22.6$ kJ/mol.

For numerical modeling of the dynamics of the macromolecule PE it is convenient to present the interaction potential by

$$W_1(\delta)=C_1\sin^2(\delta/2)+C_2Z_\beta(\delta), \tag{3}$$

where the one-parametric potential

$$Z_\beta(\delta)=\left[\frac{(1+\beta)\sin(3\delta/2)}{1-\beta\sin(3\delta/2)}\right]^2$$

describes a non-negative function of the period $4\pi/3$, having minima at the points $\delta=0,\ 2\pi/3$ [$Z_\beta(0)=Z_\beta(2\pi/3)=0$] and maxima at the points $\delta=\pi/3,\ \pi$ ($Z_\beta(\pi/3)=[(1+\beta)/(1-\beta)]^2$, $Z_\beta(\pi)=1$). The parameter $|\beta|<1$ determines the relation of the barrier heights between the potential minima (3).

The values of the parameters C_1, C_2, and β of the potential of rotation (3) are uniquely determined by the equations

$$W_1(\pi/3)=C_1/4+C_2[(1+\beta)/(1-\beta)]^2=\epsilon_1,$$

$$W_1(2\pi/3)=3C_1/4=\epsilon_2,$$

$$W_1(\pi)=C_1+C_2=\epsilon_3,$$

from which we have $C_1=4\epsilon_2/3=2.7679$ kJ/mol, $C_2=\epsilon_3-c_1=19.8338$ kJ/mol, $\beta=(\sqrt{d}-1)/(\sqrt{d}+1)=-0.0825$, where $d=(\epsilon_1-c_1/4)/c_2$. The potential (3) with the indicated values of the parameters is given in Fig. 1.

The potential of interaction for the macromolecule PTFE is also presented in Fig. 1. The difference between these potentials is connected with the polarity of the bond C—F. The other reason is that the van der Vaals radius of a fluorine atom is larger than the radius of a hydrogen atom. All this leads to additional contributions to the total potential energy of rotation compared with PE. Having three rotary isomers on each bond C—C, one with the minimal energy *(trans)* and two with higher energies [*gauche* (+) and *gauche* (−)], PTFE has four isomers. Two of them [*trans* (+) and *trans* (−)] have identical minimal energy [$\delta_1=\delta_0,\ \delta_2=2\pi-\delta_0,\ W(\delta_1)=W(\delta_2)=0$]; the other two [*gauche* (+) and *gauche* (−)] have higher energies [$\delta_3\approx2\pi/3,\ \delta_4\approx4\pi/3,\ W(\delta_3)=W(\delta_4)>0$].

The potential of rotation is characterized by four characteristics: the height of the potential barriers between both *trans* conformations $\epsilon_0=W(0)$, and between *trans* and *gauche* conformations $\epsilon_1=W(\pi/3)$, the level of the *gauche* conformation energy $\epsilon_2=W(2\pi/3)$, and the height of the barrier between *gauche* conformations $\epsilon_3=W(\pi)$. According to [21], $\epsilon_0=1.674$ kJ/mol, $\epsilon_1=18.42$ kJ/mol, $\epsilon_2=4.186$ kJ/mol, and $\epsilon_3=23.02$ kJ/mol.

For numerical modeling of the dynamics of the macromolecule PTFE it is convenient to present the potential of interaction by the formula

$$W_2(\delta)=[C_3Z_\alpha(\delta)+C_4Z_\beta(\delta)-C_5]^2, \tag{4}$$

where the one-parametric function

$$Z_\alpha(\delta)=\frac{(1+\alpha)\sin^2(\delta/2)}{1+\alpha\sin^2(\delta/2)}.$$

The parameter values $C_3=3.411$ $(\text{kJ/mol})^{1/2}$, $C_4=2.681$ $(\text{kJ/mol})^{1/2}$, $C_5=1.294$ $(\text{kJ/mol})^{1/2}$, $\alpha=14.6125$, and $\beta=4.0028\times10^{-3}$ are determined from the equations

$$W(0)=C_5^2=\epsilon_0,$$

$$W(\delta_0)=[C_3Z_\alpha(\delta_0)+C_4Z_\beta(\delta_0)-C_5]^2=0,$$

$$W(\pi/3)=\left[C_3\frac{1+\alpha}{4+\alpha}+C_4\left(\frac{1+\beta}{1-\beta}\right)^2-C_5\right]^2=\epsilon_1,$$

$$W(2\pi/3)=\left[3C_3\frac{1+\alpha}{4+3\alpha}-C_5\right]^2=\epsilon_2,$$

$$W(\pi)=(C_3+C_4-C_5)^2=\epsilon_3.$$

The potential (4) at given parameter values is presented in Fig. 1. It has an absolute minimum at $\delta=\delta_0,\ 2\pi-\delta_0$.

Let us note that the potential of rotation $W(\delta)$ for PE is symmetric with respect to the point of the absolute minimum $\delta_0=0$. The cubic anharmonicity of the potential at this point is equal to zero. For PTFE the point of the minimum δ_0 is not a point of symmetry. The cubic anharmonicity at this point is different from zero. By virtue of this, for PTFE it is possible to expect the existence of solitons of torsion stipulated by cubic anharmonicity of the rotational potential.

IV. A DISPERSION EQUATION

For the macromolecule PE the dispersion equation in the plane case was obtained by Kirkwood [23] more than 60 years ago. The dispersion equation for the out-of-plane dynamics was presented in [17]. The velocity of long-wave (longitudinal) acoustic phonons

$$v_l=2\sqrt{K_2/M}\tan(\theta_0/2)/\sqrt{1+4\varepsilon\tan(\theta_0/2)},$$

where the dimensionless parameter $\varepsilon=K_2/K_1\rho_0^2$; $K_1=2D_0\alpha^2$ is the stiffness of a valence bond and $K_2=\gamma\sin^2\theta_0$ is the stiffness of a valence angle.

The velocity of long-wave torsional phonons

$$v_t=4\delta z\sqrt{K_3/M},$$

where the stiffness coefficient $K_3=W_1''(0)\rho_0/(4R_0\delta z)^2$.

Let us find the dispersion equation for the PTFE macromolecule. It is convenient for the analysis of low-amplitude oscillations of a helix chain to pass from the cylindrical coordinates r_n, φ_n, and h_n to the local coordinates

$$\mathbf{u}_n=\begin{pmatrix}u_{n,1}\\u_{n,2}\\u_{n,3}\end{pmatrix}=\begin{pmatrix}\cos(n\Delta\phi) & \sin(n\Delta\phi) & 0\\ -\sin(n\Delta\phi) & \cos(n\Delta\phi) & 0\\ 0 & 0 & 1\end{pmatrix}\times\begin{pmatrix}(R_0+r_n)\cos(n\Delta\phi+\varphi_n)-R_0\cos(n\Delta\phi)\\(R_0+r_n)\sin(n\Delta\phi+\varphi_n)-R_0\sin(n\Delta\phi)\\h_n\end{pmatrix}.$$

In the given coordinate frame the Hamiltonian (2) has the form

$$H=\sum_n\{\tfrac{1}{2}M(\dot{\mathbf{u}}_n,\dot{\mathbf{u}}_n)+V(\mathbf{u}_n,\mathbf{u}_{n+1})+U(\mathbf{u}_{n-1},\mathbf{u}_n,\mathbf{u}_{n+1})+W(\mathbf{u}_{n-1},\mathbf{u}_n,\mathbf{u}_{n+1},\mathbf{u}_{n+2})\}. \quad (5)$$

The following equations of motion correspond to the Hamiltonian (5):

$$\begin{aligned}-M\ddot{\mathbf{u}}_n=&\mathbf{V}_1(\mathbf{u}_n,\mathbf{u}_{n+1})+\mathbf{V}_2(\mathbf{u}_{n-1},\mathbf{u}_n)+\mathbf{U}_1(\mathbf{u}_n,\mathbf{u}_{n+1},\mathbf{u}_{n+2})\\&+\mathbf{U}_2(\mathbf{u}_{n-1},\mathbf{u}_n,\mathbf{u}_{n+1})+\mathbf{U}_3(\mathbf{u}_{n-2},\mathbf{u}_{n-1},\mathbf{u}_n)\\&+\mathbf{W}_1(\mathbf{u}_n,\mathbf{u}_{n+1},\mathbf{u}_{n+2},\mathbf{u}_{n+3})\\&+\mathbf{W}_2(\mathbf{u}_{n-1},\mathbf{u}_n,\mathbf{u}_{n+1},\mathbf{u}_{n+2})\\&+\mathbf{W}_3(\mathbf{u}_{n-2},\mathbf{u}_{n-1},\mathbf{u}_n,\mathbf{u}_{n+1})\\&+\mathbf{W}_4(\mathbf{u}_{n-3},\mathbf{u}_{n-2},\mathbf{u}_{n-1},\mathbf{u}_n),\end{aligned} \quad (6)$$

where the vectors

$$\mathbf{V}_i(\mathbf{u}_1,\mathbf{u}_2)=\frac{\partial}{\partial\mathbf{u}_i}V,\quad i=1,2;$$

$$\mathbf{U}_i(\mathbf{u}_1,\mathbf{u}_2,\mathbf{u}_3)=\frac{\partial}{\partial\mathbf{u}_i}U,\quad i=1,2,3;$$

$$\mathbf{W}_i(\mathbf{u}_1,\mathbf{u}_2,\mathbf{u}_3,\mathbf{u}_4)=\frac{\partial}{\partial\mathbf{u}_i}W,\quad i=1,2,3,4.$$

The linear approach to the nonlinear equations (6) takes the form

$$\begin{aligned}-M\ddot{\mathbf{u}}_n=&B_1\mathbf{u}_\mathbf{n}+B_2(\mathbf{u}_{\mathbf{n}-1}+\mathbf{u}_{\mathbf{n}+1})+B_3(\mathbf{u}_{\mathbf{n}-2}+\mathbf{u}_{\mathbf{n}+2})\\&+B_4(\mathbf{u}_{\mathbf{n}-3}+\mathbf{u}_{\mathbf{n}+3}),\end{aligned} \quad (7)$$

where the constants of the matrices are determined by the relations

$$B_1=V_{11}+V_{22}+U_{11}+U_{22}+U_{33}+W_{11}+W_{22}+W_{33}+W_{44},$$

$$B_2=V_{12}+U_{12}+U_{23}+W_{12}+W_{23}+W_{34},$$

$$B_3=U_{13}+W_{13}+W_{24},$$

$$B_4=W_{14}.$$

Here,

$$V_{ij}=\frac{\partial^2V}{\partial\mathbf{u}_i\,\partial\mathbf{u}_j}(\mathbf{0},\mathbf{0}),\quad i,j=1,2;$$

$$U_{ij}=\frac{\partial^2U}{\partial\mathbf{u}_i\,\partial\mathbf{u}_j}(\mathbf{0},\mathbf{0},\mathbf{0}),\quad i,j=1,2,3;$$

$$W_{ij}=\frac{\partial^2W}{\partial\mathbf{u}_i\,\partial\mathbf{u}_j}(\mathbf{0},\mathbf{0},\mathbf{0},\mathbf{0}),\quad i,j=1,2,3,4.$$

Let us look for the solution of the linear system (7) in the form of the harmonic wave

$$\mathbf{u}_n=\mathbf{A}\exp[i(qn-\omega t)]. \quad (8)$$

After the substitution of the expression (8) into the linear equation (7) we obtain the dispersion equation

$$|B_1+2\cos(q)B_2+2\cos(2q)B_3+2\cos(3q)B_4-\omega^2E|=0, \quad (9)$$

where E is the unit matrix.

The dispersion equation (9) is an algebraic equation of the third order with respect to the variable ω^2. The corresponding algebraic curve has three branches: two acoustic $\omega=\omega_t(q)$, $\omega=\omega_l(q)$ and one optical $\omega=\omega_o(q)$ [$\omega_t(q)\leqslant\omega_l(q)\leqslant\omega_o(q)$]. The dispersion curves are given in Fig. 2. The lower curve $\omega=\omega_t(q)$ gives the dispersion law for acoustic phonons corresponding to torsional oscillations, and the medial curve $\omega=\omega_l(q)$ the dispersion law for acoustic phonons corresponding to longitudinal oscillations of the helix. The upper curve $\omega=\omega_o(q)$ corresponds to high-frequency optical phonons of the helix.

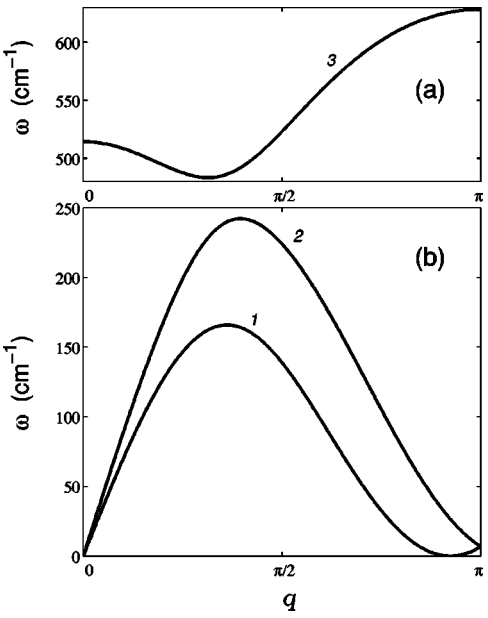

FIG. 2. The frequency spectrum curves $\omega=\omega_t(q)$ (1), $\omega=\omega_l(q)$ (2), and $\omega=\omega_o(q)$ (3), for the spiral isolated macromolecule PTFE.

The velocity of long-wave longitudinal phonons

$$v_l=\Delta z \lim_{q\to 0}\frac{\omega_l(q)}{q}=6978.6 \text{ m/s}$$

exceeds the velocity of torsional phonons

$$v_t=\Delta z \lim_{q\to 0}\frac{\omega_t(q)}{q}=5585.3 \text{ m/s}.$$

The ratio of the velocities is $s_t=v_t/v_l=0.800\,35$.

V. NUMERICAL METHOD OF FINDING NONLINEAR SOLITARY WAVES

The equations of motion that correspond to the Hamiltonian (2) have the form

$$M\ddot{r}_n-M(R_0+r_n)\dot{\varphi}_n^2+\frac{\partial}{\partial r_n}P=0,$$

$$M(R_0+r_n)^2\ddot{\varphi}_n+2M(R_0+r_n)\dot{\varphi}_n\dot{r}_n+\frac{\partial}{\partial \varphi_n}P=0, \quad (10)$$

$$M\ddot{h}_n^2+\frac{\partial}{\partial h_n}P=0,$$

where the potential energy

$$P=\sum_n \{V(\rho_n)+U(\theta_n)+W(\delta_n)\}.$$

The complexity of the equations of motion does not allow us to study them analytically, therefore for the analysis of soliton solutions we will take advantage of a numerical method [7].

The solution of Eqs. (10) will be searched for as a traveling solitary smooth wave of a constant profile. For this purpose let us assume $r_n(t)=r(\xi)$, $\varphi_n(t)=\varphi(\xi)$, and $h_n(t)=h(\xi)$, where the wave variable $\xi=n\Delta z-vt$, v is the wave velocity, and the functions r, φ, and h smoothly depend on ξ.

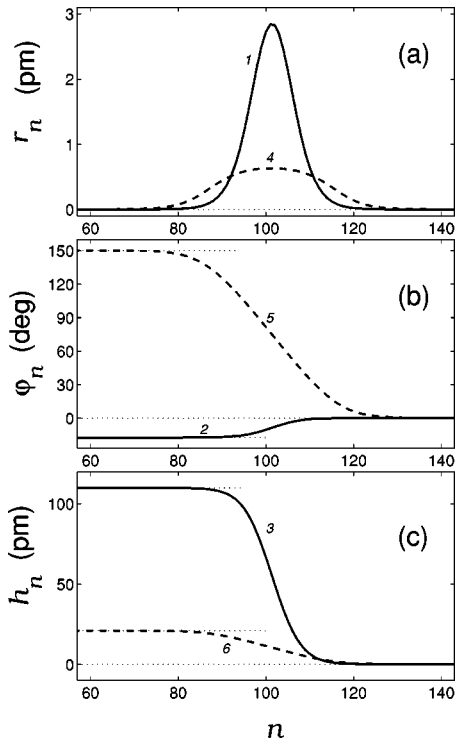

FIG. 3. The profiles of the soliton of longitudinal compression (components r_n, φ_n, h_n, curves 1, 2, 3) at velocity $s=1.02$ and the soliton of torsion (curves 4, 5, 6) at velocity $s=0.82$.

Using the discrete approximations of time derivatives

$$\dot{r}_n=-v(r_{n+1}-r_{n-1})/2\Delta z,$$

$$\dot{\varphi}_n=v(\psi_{n+1}-5\psi_n-2\psi_{n-1})/6\Delta z,$$

$$\ddot{r}_n=v^2(r_{n+1}-2r_n+r_{n-1})/\Delta z^2,$$

$$\ddot{\varphi}_n=-v^2(\psi_{n+1}-15\psi_n+15\psi_{n-1}-\psi_{n-2})/12\Delta z^2,$$

$$\ddot{h}_n=-v^2(w_{n+1}-15w_n+15w_{n-1}-w_{n-2})/12\Delta z^2,$$

where the relative rotational displacement $\psi_n=\varphi_{n+1}-\varphi_n$ and the relative displacement $w_n=h_{n+1}-h_n$, we write the equations of motion (10) as a system of discrete equations in variables r_n, ψ_n, w_n:

$$F_{1,n}=-c_1(r_{n+1}-2r_n+r_{n-1})+c_2(\psi_{n+1}-5\psi_n-2\psi_{n-1})^2\times(R_0+r_n)+F_1(r_{n-3},\ldots,r_{n+3};\psi_{n-3},\ldots,\psi_{n-2};w_{n-3},\ldots,w_{n+2})=0,$$

$$F_{2,n}=c_3(\psi_{n+1}-15\psi_n+15\psi_{n-1}-\psi_{n-2})+c_4(r_{n+1}-r_{n-1})\times(\psi_{n+1}-5\psi_n-2\psi_{n-1})/(R_0+r_n)+F_2(r_{n-3},\ldots,r_{n+3};\psi_{n-3},\ldots,\psi_{n-2};w_{n-3},\ldots,w_{n+2})=0, \quad (11)$$

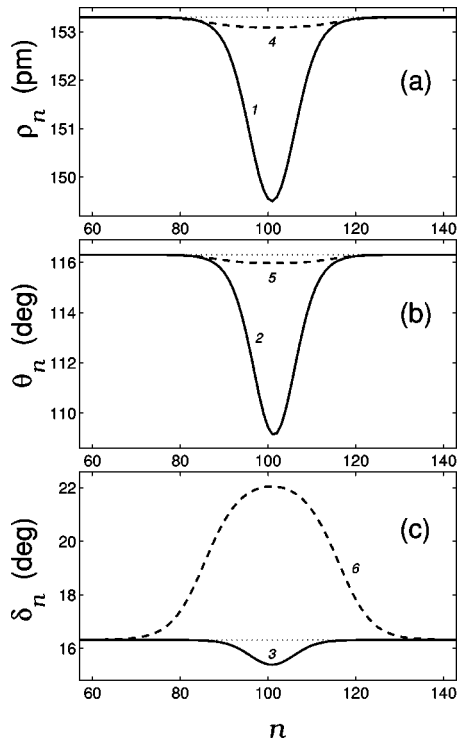

FIG. 4. Change of length of the valence bonds ρ_n, valence angle θ_n, and conformational angles δ_n in the localization region of the soliton of compression (curves 1, 2, 3) at velocity $s=1.02$ and the soliton of torsion (curves 4, 5, 6) at $s=0.82$.

$$F_{3,n}=c_3(w_{n+1}-15w_n+15w_{n-1}-w_{n-2}) +F_3(r_{n-3},\ldots,r_{n+3};\psi_{n-3},\ldots,\psi_{n-2}; w_{n-3},\ldots,w_{n+2})=0,$$

where the coefficients $c_1=v^2/\Delta z^2$, $c_2=c_1/36$, $c_3=c_1/12$, and $c_4=c_1/6$.

We search numerically for soliton solutions $\{r_n,\psi_n,w_n\}_{n=1}^N$ for discrete systems of Eqs. (11) as solutions of the problem for a conditional minimum,

$$F=\frac{1}{2}\sum_{n=2}^{N-1}(F_{1,n}^2+F_{2,n}^2+F_{3,n}^2)\rightarrow\min, \qquad r_1=r_N=\psi_1=\psi_N=w_1=w_N=0. \tag{12}$$

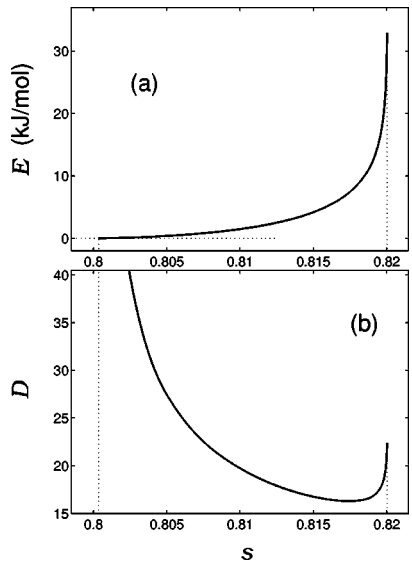

FIG. 5. Dependence of the energy E (a), and width D (b) of the soliton of torsion on the dimensionless velocity s.

The solution of this problem allows us to find numerically all soliton solutions (solitary waves of a constant profile) for the equations of motion (10). The absence of such solutions at any value of v means the impossibility of soliton motion at this value of velocity.

The problem (12) was solved numerically by the method of conjugate gradients. The solution was searched for in the chains with $N=400$ bonds (the given value N ensures the independence of the shape of the solution of zero boundary conditions). The initial point of descent was taken in the form of three symmetric bell-shaped profiles $r(n)$, $\psi(n)$, and $w(n)$ centered at the middle of the chain.

Each soliton solution $\{r_n,\psi_n,w_n\}_{n=1}^N$ is characterized by the energy

$$E=\sum_{n=2}^{N-1}\left(\frac{Mv^2}{8\Delta z^2}[(r_{n+1}-r_{n-1})^2+(R_0+r_n)^2(\psi_n+\psi_{n-1})^2 +(w_n+w_{n-1})^2]+V(\rho_n)+U(\theta_n)+W(\delta_n)\right),$$

the total torsion

TABLE I. Dependence of the energy E, width D, total compression R, torsion Ψ, and amplitudes A_r, A_ρ, A_θ, A_δ of the soliton of torsion on the dimensionless velocity s.

s	E (kJ/mol)	D	R (pm)	Ψ (deg)	A_r (pm)	A_ρ (pm)	A_θ (deg)	A_δ (deg)
0.8025	0.11	39.9	−1.2	−11.8	0.03	−0.01	−0.006	0.32
0.8050	0.37	27.5	−1.9	−18.5	0.06	−0.02	−0.017	0.72
0.8075	0.81	22.5	−2.6	−24.6	0.10	−0.03	−0.033	1.16
0.8100	1.48	19.7	−3.3	−31.1	0.14	−0.05	−0.052	1.65
0.8125	2.51	17.9	−4.3	−38.6	0.20	−0.07	−0.080	2.21
0.8150	4.19	16.8	−5.6	−48.4	0.28	−0.10	−0.120	2.88
0.8175	7.47	16.3	−7.9	−64.0	0.38	−0.13	−0.179	3.77
0.8200	28.61	21.0	−20.1	−144.8	0.63	−0.21	−0.325	5.70

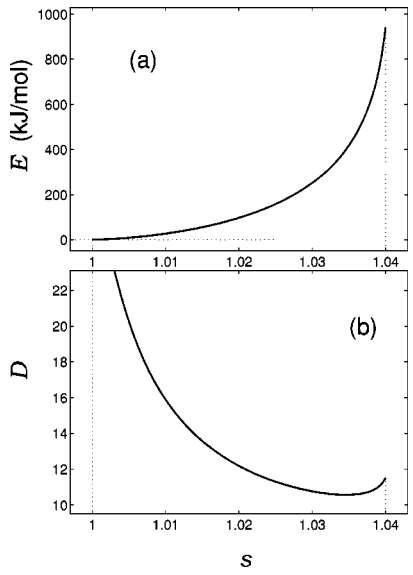

FIG. 6. Dependence of the energy E (a) and width D (b) of the soliton of compression on the dimensionless velocity s.

$$\Psi = \sum_{n=1}^{N} \psi_n ,$$

and the compression of the chain

$$R = \sum_{n=1}^{N} w_n .$$

The mean-squared width of the soliton measured in the periods of the chain is written as

$$D = 2\left[\sum_{n=1}^{N} (n-\overline{n}) w_n \Big/ R \right]^{1/2},$$

where $\overline{n} = \Sigma_{n=1}^{N} n w_n / R$ gives the position of the soliton center. The solution is also characterized by the amplitude of transverse displacements of the bonds of the helix backbone $A_r = \max_n r_n$, the amplitudes of the strain of valence bonds $A_\rho = \min_n(\rho_n - \rho_0)$, of the valence angles $A_\theta = \min_n(\theta_n - \theta_0)$, and of the angles of rotation $A_\delta = \max_n(\delta_n - \delta_0)$.

TABLE II. Dependence of the energy E, width D, total compression R, torsion Ψ, and amplitudes A_r, A_ρ, A_θ, A_δ of the soliton of longitudinal compression on the dimensionless velocity s.

s	E (kJ/mol)	D	R (pm)	Ψ (deg)	A_r (pm)	A_ρ (pm)	A_θ (deg)	A_δ (deg)
1.005	8.8	20.3	−44	7.8	0.6	−1.0	−1.6	−0.3
1.010	27.8	15.9	−66	11.4	1.3	−1.9	−3.3	−0.5
1.015	55.5	13.6	−88	14.5	2.0	−2.8	−5.1	−0.7
1.020	97.2	12.2	−110	17.4	2.8	−3.8	−7.2	−0.9
1.025	158.3	11.3	−135	20.5	3.8	−4.8	−9.5	−1.1
1.030	252.4	10.8	−165	24.3	4.9	−5.9	−12.2	−1.3
1.035	418.6	10.6	−211	29.9	6.2	−7.1	−15.8	−1.5
1.040	941.0	11.5	−334	44.9	8.5	−8.8	−21.8	−1.7

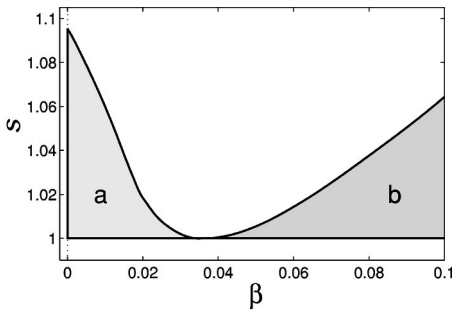

FIG. 7. Existence region for acoustic supersonic solitons of tension (a) and solitons of compression of the *trans* zigzag in the space of dimensionless parameters β and s.

VI. DYNAMIC PROPERTIES OF SOLITONS

Numerical solution of the problem (12) has shown the existence of soliton solutions of two types. The first solution describes the propagation of a torsional solitary wave along the PTFE chain. The typical form of the solution is presented in Fig. 3. The displacements of all three components r_n, φ_n, and h_n have the form of a solitary wave. In combination they

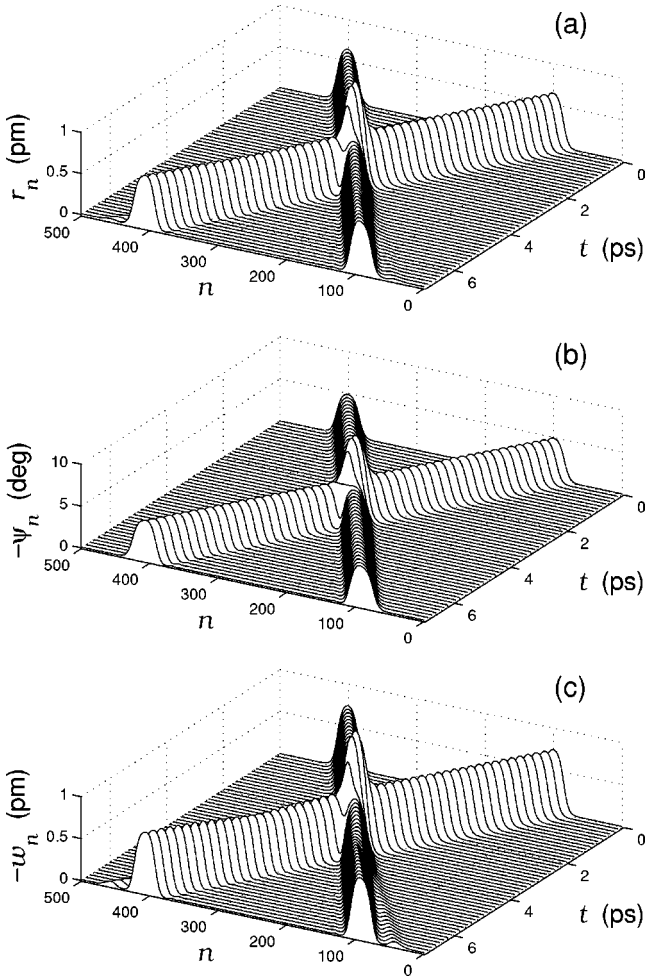

FIG. 8. Collision of solitons of torsion ($s = 0.82$) in the helix of PTFE. The dependence of transversal displacement r_n (a), relative rotation ψ_n (b), and relative longitudinal displacement w_n (c) on the number of the bond n and time t. The radiation of phonons with respect to component w_n can be seen.

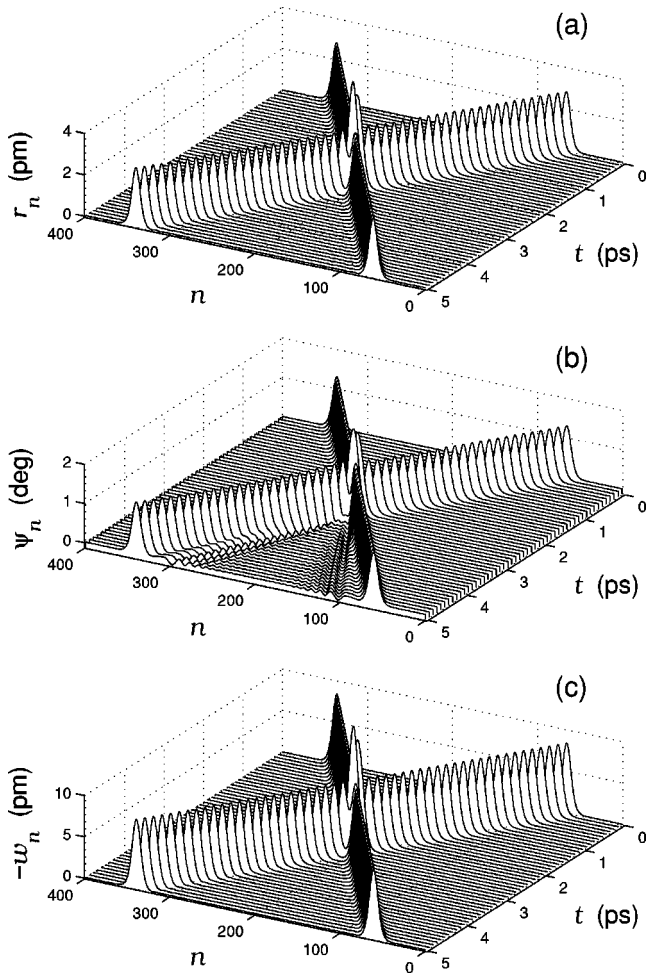

FIG. 9. Inelastic collision of solitons of torsion ($s=1.02$) in the helix of PTFE. The radiation of phonons with respect to component ψ_n can be seen.

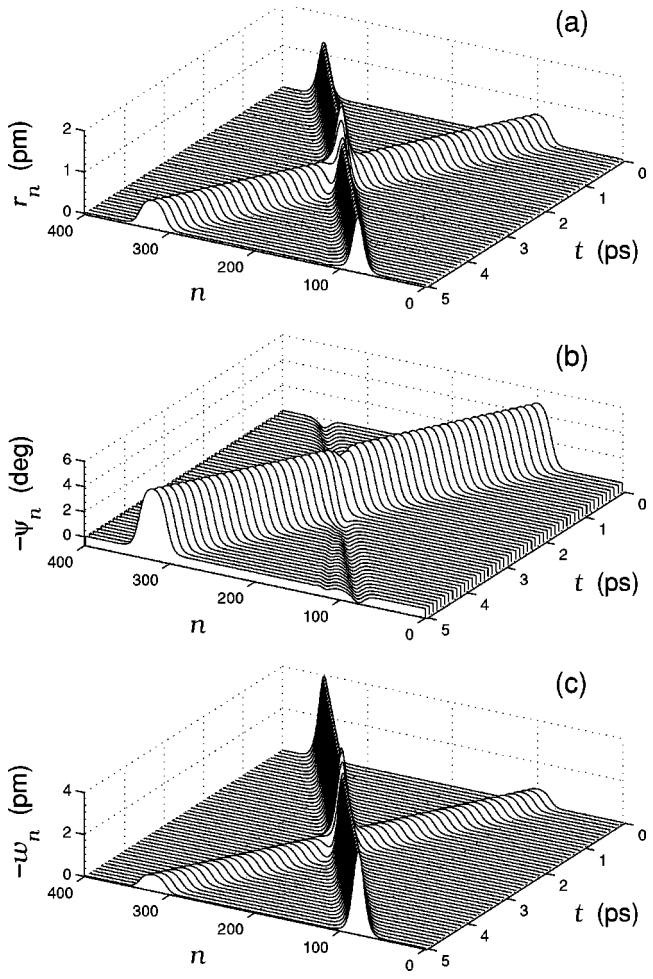

FIG. 10. Collision of the soliton of torsion ($s=0.82$) with the solitons of longitudinal compression ($s=-1.01$) in the helix of PTFE.

describe a localized torsion of the helix. In the region of localization of the soliton on the transverse component r_n the helix is expanded, on the angular variable φ_n monotonically twisted, and on the longitudinal direction h_n monotonically squeezed. As is visible from Fig. 4, all these deformations of the helix are achieved basically by the expense of local magnification of the rotation angles δ_n, i.e., by the expense of squeezing dihedral angles of a chain.

The second solution describes the propagation of a solitary wave of longitudinal compression. The form of the solution is given in Fig. 3. The displacements of the three components r_n, φ_n, and h_n also have the form of a solitary wave, but in combination they describe a localized longitudinal compression of the helix. In the region of localization of the soliton on the transverse component r_n the helix is expanded, on the angular variable φ_n slightly untwisted, and on the longitudinal direction h_n squeezed. From Fig. 4 it is visible that these deformations are reached first of all at the expense of squeezing the valence angles and valence bonds. Thus the torsional angles are weakly deformed.

The solitons of torsion have the finite interval of permissible values of dimensionless velocity $s_t<s<0.820\,034$, where the dimensionless velocity $s=v/v_l$. The dependencies of the energy E and width D of the soliton on the dimensionless velocity s are presented in Fig. 5. With the growth of the velocity, the soliton energy monotonically increases and the width monotonically decreases up to the minimum value $D=16.3$ at $s=0.818$ and then begins to grow monotonically. Concrete values of the energy E, width D, total compression R, torsion of the spiral Ψ, amplitude of transversal expansion of the chain A_r, and extreme values of strains of valence bonds A_ρ, of valence angles A_θ, and of angles of rotation A_δ are presented in Table I. As follows from this table, the amplitude of longitudinal compression of the chain grows monotonically with the growth of velocity and reaches the maximum value -23 pm at the maximum value of the velocity. The transversal expansion of the helix does not reach an essential value. At all values of the velocity the valence bonds and the angles are almost undeformed, as against the angles of rotation. The amplitude of deformation of torsion angles monotonically grows with growth of velocity. The maximum deformation happens on the right end of the interval of velocities, where the total torsion of the helix $\Psi=-163.5°$.

The solitons of compression of the helix have an interval of permissible values of dimensionless velocity $1<s<1.04$. The dependencies of energy E and width D of the soliton on s are presented in Fig. 6. The energy of the soliton grows monotonically with growth of the velocity and the width monotonically decreases up to the minimum value D

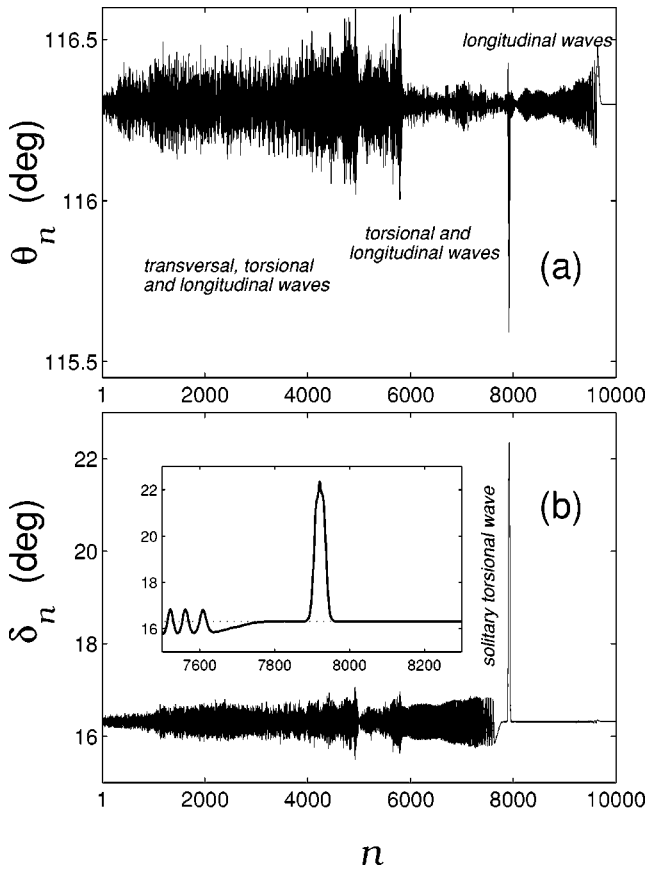

FIG. 11. The formation of the soliton of torsion and three wave packets in the helix macromolecule PTFE at compression of 40° of the first dihedral angle; the dependence of the valence angles θ_n (a) and angles of rotation δ_n (b) on the number of bond n for time $t = 180$ ps.

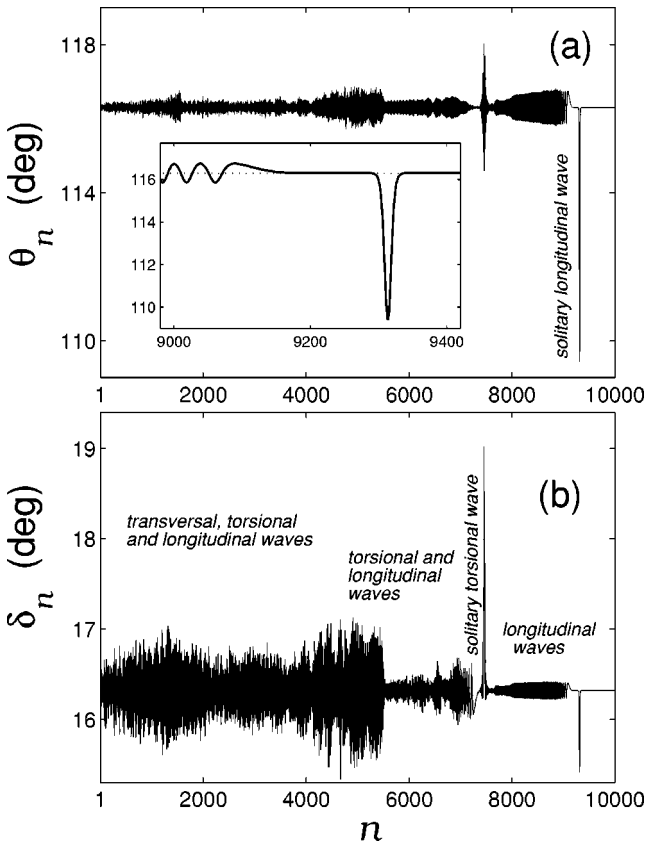

FIG. 12. The formation of the soliton of torsion, the soliton of longitudinal compression, and three wave packets in the helix macromolecule PTFE at compression of 40° of the first valence angle (time $t = 170$ ps).

$=10.19$ at $s=1.035$ and then begins to grow monotonically. Concrete values of energy E, width D, total compression R, and torsion of the helix Ψ, the amplitude of transverse expansion of the chain A_r, and extreme values of the strain of valence bonds A_ρ, valence angles A_θ, and angles of rotation A_δ are presented in Table II. The amplitude of longitudinal compression of the chain grows monotonically with growth of the velocity and reaches the maximal value 0.334 nm on the right end of the interval of velocities. The amplitude of transverse expansion can reach the value 8.5 pm, which exceeds by more than one order of magnitude the maximum value of expansion of the helix for a soliton of torsion. Large values can also be reached by the strains of the valence bonds and angles. The dihedral angles thus are weakly deformed. So the tension of a torsion angle at the maximum value of velocity does not exceed 1.7°.

An analysis of soliton dynamics in a plane zigzag PE chain was made in [16], in which the lower value of the maximum energy of strain of a valence angle $K_\theta = 130.122$ kJ/mol [22] was used. It was shown that a soliton of tension with a narrow supersonic velocity spectrum can exist in the *trans* zigzag chain. It is interesting to consider the dependence of the solution on the value of the dimensionless parameter

$$\beta = K_2 / K_1 \rho_0^2,$$

where

$$K_1 = \frac{d^2}{d\rho^2} V(\rho)\bigg|_{\rho=\rho_0} = 2D_0\alpha^2$$

is the stiffness of the valence bond and

$$K_2 = \frac{d^2}{d\theta^2} U(\theta)\bigg|_{\theta=\theta_0} = K_\theta \sin^2\theta_0$$

the stiffness of the valence angle.

Numerical solution of the problem (12) has shown that only one type of acoustic soliton, namely, the soliton wave of longitudinal deformation, can exist in a plane zigzag chain. The type of soliton solution depends on the dimensional parameter β, which characterizes the relation of physical and geometrical anharmonicity of the zigzag chain. The physical anharmonicity is caused by the potential of the valence bond, and the geometrical anharmonicity by the potential of the valence angle. At values $\beta < 0.0356$ the geometrical anharmonicity plays the main role by virtue of which the soliton solution of the equations of motion corresponds to a solitary wave of tension in the plane zigzag. At $\beta > 0.0356$ the physical anharmonicity will be greater, by virtue of which the soliton solution already corresponds to a solitary wave of compression.

The dependence of the interval of soliton velocities on the parameter β is presented in Fig. 7. If $\beta<\beta_0=0.0356$, the soliton is a solitary wave of tension, and when $\beta>\beta_0$ a solitary wave of compression. In chains with $\beta=0$ (the approximation of an infinitely rigid valence bond) the soliton has the velocity spectrum $1<s<s_1=1.095$. With growth of β, the maximum value of velocity s_1 decreases monotonically. At the threshold value $\beta=\beta_0$ full compensation of geometrical and physical anharmonicity occurs and the velocity spectrum disappears ($s_1=1$). Further growth of β leads to monotonic growth of the velocity spectrum.

At the value of energy $K_\theta=130.122$ kJ/mol the dimensionless parameter $\beta=0.019\,29<\beta_0$. The soliton corresponds to a solitary wave of tension and has velocity spectrum $1<s<1.02$. At the selected value of the energy $K_\theta=529$ kJ/mol the dimensionless parameter $\beta=0.078\,419>\beta_0$. The soliton corresponds to a solitary wave of compression and has velocity spectrum $1<s<1.035$.

VII. NUMERICAL MODELING OF SOLITON DYNAMICS

Modeling of the dynamics of solitons in the chains PE and PTFE has shown their stability at all permissible values of velocity. The solitons move along a chain with a stationary value of velocity and maintain their shape.

The collision of solitons is not elastic and can be accompanied by the radiation of phonons. The solitons of torsion of spiral PTFE interact in practice as elastic particles. Their collision is accompanied by very weak radiation of longitudinal phonons only near the maximum value of velocity $s=0.82$ (Fig. 8). The collision of the solitons of longitudinal compression in the spiral is accompanied by the radiation of torsional phonons (Fig. 9). The collision of the torsional soliton with solitons of compression happens almost without the radiation of phonons (Fig. 10).

In a finite chain, supersonic solitons can arise only on its ends. We model the formation of a soliton by strain of the end of the chain. Let us consider the propagation of an initial excitation, given as deformation of the first bond, in the finite helix chain ($N=10\,000$) modeling the PTFE molecule. For this purpose we integrate numerically the equations of motion (10) with initial strain corresponding to diminution of the first dihedral angle of the chain of $\delta_1=40°$ and with strain compression of the first valence angle of $\theta_1=40°$.

The strain of the first dihedral angle leads to formation in the helix of a torsional soliton, which propagates with the greatest possible velocity $s=0.82$ (Fig. 11). Three wave packets are also formed in the chain. The first packet is formed by optical phonons, the second by supersonic phonons of torsion, and the third by longitudinal supersonic phonons. The wave packet of longitudinal supersonic phonons moves faster than the soliton. As is visible from Fig. 11, the phonons do not affect the dynamics of the torsional soliton. A soliton having velocity higher than the velocity of the torsional phonons advanced the wave packet of torsional phonons.

The compression of the first valence angle leads to the formation of two supersonic solitons (Fig. 12). The soliton of compression moves with the greatest possible velocity $s=1.04$ ahead of a wave packet of longitudinal supersonic phonons. The soliton of torsion moves also with its greatest possible velocity $s=0.82$, ahead of a wave packet of torsional phonons.

Modeling shows that the strain of the end of a spiral macromolecule can lead to the formation of two types of supersonic soliton (torsional and longitudinal compression of the helix), having supersonic intervals of velocities. It confirms the results obtained by the numerical solution of the problem (12).

VIII. CONCLUSIONS

The examination of the nonlinear dynamics of PTFE carried out allows us to conclude that in an isolated polymeric macromolecule having the shape of a three-dimensional helix there can simultaneously exist two types of supersonic soliton: solitons of torsion and solitons of longitudinal compression of the spiral. The solitons of the first type correspond to a solitary wave of rotary displacements, and solitons of the second type to a solitary wave of longitudinal displacements of the bonds. Thus intertwisting of a spiral is mainly realized as the compression of the dihedral angles, and longitudinal compression by compression of the valence angles and bonds. The solitons have finite supersonic intervals of velocities: the soliton of torsion has velocity higher than long-wave phonons of torsion, and the soliton of compression a velocity higher than the velocities of long-wave longitudinal phonons.

In the plane zigzag macromolecule PE only one type of supersonic soliton, namely, the soliton of longitudinal compression of the chain, can exist. This allows us to conclude that helicity of the polymeric macromolecule is a necessary condition for the existence in it of solitons of torsion caused by anharmonicity of the potential of interaction.

Both such supersonic solitons are dynamically stable at all possible values of the velocity and have particlelike properties (inelasticity of their interaction is exhibited only at the maximal values of the velocity). Let us note that the study of torsional solitons in isolated helix chains has to be augmented by investigation of them in a realistic nonlinear model taking into account intermolecular interaction.

ACKNOWLEDGMENT

This work was supported by the Russian Foundation of Basic Research (Grant No. 98-03-33366a).

[1] A. R. Bishop, J. A. Krumhansl, and S. E. Trullinger, Physica D **1**, 1 (1980).
[2] A. Collins, Adv. Chem. Phys. **53**, 225 (1983).
[3] A. S. Davydov, *Solitons in Molecular Systems* (Reidel, Dordrecht, 1985).
[4] A. C. Scott, Phys. Rep. **217**, 1 (1992).
[5] S. Yomosa, Phys. Rev. A **32**, 1752 (1985).
[6] P. Perez and N. Theodorakopoulos, Phys. Lett. A **117**, 405 (1986).
[7] P. L. Christiansen, A. V. Zolotaryuk, and A. V. Savin, Phys. Rev. E **56**, 877 (1997).
[8] E. Fermi, J. Pasta, and S. Ulam, *Collected Works of Enrico*

Fermi (University of Chicago Press, Chicago, 1965), Vol. II, p. 978.
[9] N. J. Zabusky and M. D. Kruskal, Phys. Rev. Lett. **15**, 241 (1965).
[10] N. J. Zabusky, Comput. Phys. Commun. **5**, 1 (1973).
[11] M. Toda, Phys. Rep. **18**, 1 (1975).
[12] O. H. Olsen, P. S. Lomdahl, and W. C. Kerr, Phys. Lett. A **136**, 402 (1989).
[13] P. S. Lomdahl, O. H. Olsen, and M. R. Samuelsen, Phys. Lett. A **152**, 343 (1991).
[14] N. I. Pahomova, L. I. Manevitch, V. V. Smirnov, and S. V. Riapusov, Sov. J. Chem. Phys. **8**, 918 (1991).
[15] L. I. Manevitch, L. S. Zarkhin, and N. S. Enikolopyan, J. Appl. Polym. Sci. **39**, 2245 (1990).
[16] L. I. Manevitch and A. V. Savin, Phys. Rev. E **55**, 4713 (1997).
[17] A. V. Savin and L. I. Manevitch, Phys. Rev. B **58**, 11 386 (1998).
[18] F. Zhang, Phys. Rev. E **56**, 6077 (1997).
[19] F. Zhang, Phys. Rev. B **59**, 792 (1999).
[20] M. Kimming, G. Strobl, and B. Stuhn, Macromolecules **27**, 2481 (1994).
[21] B. Wunderlich, *Macromolecular Physics* (Academic Press, New York, 1973), Vol. 1.
[22] B. G. Sumpter, D. W. Noid, G. L. Liang, and B. Wunderlich, Adv. Polym. Sci. **116**, 29 (1994).
[23] J. G. Kirkwood, J. Chem. Phys. **7**, 506 (1939).